

Analysis on load-bearing contact characteristics of face gear tooth surface wear

Xian-Long Peng*, Fan Zhang

College of Mechanical Engineering, Xi'an University of Science and Technology, Xi'an, China

*Corresponding Author.

Abstract

Face gear transmission is widely used in aerospace shunt-confluence transmission system. Tooth surface wear is one of the main factors affecting its bearing transmission performance and failure mode. In order to study the wear mechanism of face gear tooth surface, based on tooth contact analysis (TCA) numerical method and Archard wear theory, the UMESHMOTION subroutine in ABAQUS was developed, combining with ALE adaptive mesh technology, the finite element mesh wear model of face gear pair was established. By solving the load-bearing contact problems of worn face gear pair, the load distribution coefficient among gear tooth, tooth root bending stress, tooth surface contact stress and loaded transmission error were obtained. The result shows that the tooth root wear is the most serious and the wear at the pitch cone is close to 0. The wear law of tooth surface along tooth width direction is convex parabola and the wear law along tooth height direction is concave parabola. Moderate tooth surface wear improves the bearing contact performance of face gear.

Key words: face gear, tooth surface wear, Archard wear theory, UMESHMOTION subroutine.

I. INTRODUCTION

Face gear transmission [1] is an angle transmission mechanism composed of involute cylindrical gear and bevel gear. Face gear transmission has the advantages of small transmission error amplitude, high transmission efficiency and large transmission coincidence degree. It is widely used in the key transmission systems of helicopters and high performance vehicles. Due to the contact pressure between the tooth surfaces and the relative sliding velocity along the tooth width and tooth height direction, the tooth surface wear of the face gear will inevitably occur in the mesh process, and excessive wear will bring large impact vibration, which will cause tooth failure in severe cases. Therefore, it is necessary to clarify the wear distribution law of face gear tooth surface and the specific influence of wear on bearing transmission performance.

The theoretical research on gear wear was mainly based on the quasi-static numerical method [2-4] of Archard wear model to calculate wear. The specific parameters such as load [5] and wear coefficient [6] in the model were corrected and improved by scholars, so as to predict the wear life [7] and put forward the

corresponding anti-wear method[8].The experimental study of tooth surface wear explored the influences of specific parameters such as load, rotational speed, lubricant temperature and surface roughness on tooth surface wear through wear experiments[9],and then measured the wear coefficients of gear tooth in Archard wear model under different working conditions and surface conditions[10].Some scholars carried out comparative wear tests to prove that tooth shape optimization design can achieve certain anti-wear effect[11].

Combining Archard wear model with the finite element contact model of quasi-hyperbolic gear, Park D first calculated the sliding distance and contact pressure along the contact areas at each rotating positions. According to the kinematics and geometry theory of quasi-hyperbolic gear tooth surface, the sliding distance along the contact area was calculated. The contact model was used to calculate the vertical contact stress distribution, and the influences of gear positions error on different wear types were verified[12].Then he proposed a semi-analytical contact algorithm to improve the computational efficiency of slip distance, contact pressure and tooth wear[13]. Finally he proposed an approximate and fast calculation method for the tooth surface wear of quasi-hyperbolic gear. Combined with the tooth surface load obtained from the semi-analytical method and the Archard wear model, the surface interpolation method was used to calculate the tooth surface wear, and the results of this model were compared with those of the semi-analytical method[14].

Although the numerical method for solving the wear problem of face gear can effectively shorten the calculation time, it cannot accurately express the wear distribution of face gear tooth surface, nor can it explain the specific influence of wear on the bearing transmission performance of face gear. Based on tooth contact analysis (TCA) and Archard wear theory, the UMESHMOTION subroutine in ABAQUS was developed, combining with ALE adaptive mesh technology, the finite element mesh wear model of face gear pair was established.The tooth surface wear distribution of face gear was calculated, and the load-bearing contact problem of worn face gear pair was solved.

II. FACE GEAR TOOTH SURFACE WEAR SIMULATION

2.1 Establishment of the finite element model of face gear pair

Table 1 shows the transmission parameters of face gear pair.

TABLE1. Face gear pair transmission parameters

Face gear transmission parameters	Value
number of pinion teeth	25
number of hypothetical pinion teeth	28
number of face gear teeth	160
pressure angle/ (°)	25
axes-angle/ (°)	90
gear module	6.35

pinion tooth width/mm	80
face gear tooth width/mm	80
face gear inner diameter/mm	480
Face gear outer diameter/mm	560

The discrete data points of pinion and face gear tooth surfaces were obtained by numerical calculation, and the tooth nodes were obtained by rotating the discrete data points array around their axes[15]. We numbered the grid model nodes according to ABAQUS rules and multi-tooth models were obtained by rotating the generated single tooth mesh models around their axes. Considering the influence of coincidence degree, we decided to use the five-tooth model.

According to the geometric transmission error image output by tooth contact analysis (TCA), the input rotation angle of gear pair in finite element analysis was corrected[16]. The five-tooth model was assembled into TCA fixed coordinate system by dispersing rotation angle[17]. The nodes' data and elements' data of the five-tooth model in the coordinate system was written into the inp file of each rotation angle. The finite element pre-processing settings of face gear were also written in the inp file, and the specific settings were shown in Reference[16]. Figure1 shows the finite element mesh model of face gear pair.

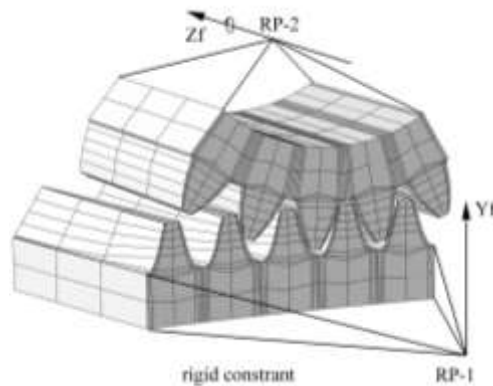


Figure1. Finite element mesh model of face gear pair(unrefined mesh)

2.2 Archard wear model in finite element analysis

When a pair of gears engage, there are both rotations and slides between the two tooth surfaces, moreover, the curvature and the load of contact position is time-varying. For such contact surface wear, Archard wear formula can be used to calculate, and its mathematical expression is as follows:

$$V = K \frac{W}{H} s \tag{1}$$

V is the volume wear of the material ; s is the sliding distance; K is dimensionless wear coefficient of contact surface ; W is vertical contact stress; H is the material hardness of observation surface.

Applying Archard model to local small area areas, formula (1) can be changed to:

$$h = kp\Delta s \tag{2}$$

h is wear depth ; $k = K / H$ is dimensional wear coefficient ; p is contact pressure ; Δs is relative sliding displacement ; wear coefficient $k = 1.0 \times 10^{-13} \text{mm}^2 / \text{N}$ was obtained by Anders and Flodin[18] in the wear test of spur gear.

When ABAQUS UMESHMOTION subroutine is used for wear finite element analysis, the continuous wear process is dispersed by the subroutine, and the wear process is divided into multiple cumulative wear increments. In each small increment step, the pressure and wear coefficient at the contact point do not change. The wear depth of node i is as follows:

$$h_{i,m} = h_{i,m-1} + kp_{i,m}\Delta s_{i,m} \quad (3)$$

$h_{i,m}$ is the total wear depth of node i at the increment step m ; $h_{i,m-1}$ is the total wear depth of node i at the increment step $m-1$; $p_{i,m}$ is the contact pressure of node i at the increment step m ; $\Delta s_{i,m}$ is the relative sliding displacement increment of node i at the increment step m .

In order to reduce the computational cost, we assumed that each gear engagement causes the same amount of wear at node i in the same mesh circle . The total wear depth can be written as follows:

$$h_{i,m} = h_{i,m-1} + \Delta Nkp_{i,m}\Delta s_{i,m} \quad (4)$$

ΔN is gear pair engagement times in each mesh circle.

2.3 Update of geometric characteristics of wear region in finite element analysis

When ABAQUS UMESHMOTION subroutine is used for wear finite element analysis, after each incremental step calculation is completed, the contact node will move to a certain extent according to the wear depth calculated by using Archard wear model in each incremental step. The corresponding positions of the nodes will be updated according to the wear depth, and the nodes' default moving direction is vertical .In order to avoid the grid distortion caused by excessive nodes movement, the contact elements grid will be redrawn when the node positions are updated by using the Arbitrary Lagrangian-Eulerian (ALE) adaptive grid technology in ABAQUS. When the main program completes the contact element grid redrawing task, the UMESHMOTION subroutine will be used for the wear calculation of the next incremental step. ALE adaptive grid technology combines the characteristics of pure Lagrange and Euler algorithm, which can make the grid flow independently from the material. Without changing the original topology of the grid, it can effectively ensure the grid quality in the analysis process[19].

2.4 Pre-processing and post-processing setting steps of wear finite element

On the basis of reference[16] ,we simulated the mesh wear process of the face gear transmission by using ABAQUS implicit static analysis method, that is, the tooth surface wear of face gear is the sum of tooth surface wear of face gear in p models.

The contact surface was set to be finite sliding face-to-face contact in each rotation in p models. Face gear tooth surface was set to be slave surface. Pinion tooth surface was set to be master surface. The observed tooth surface of face gear was set as ALE area to calculate tooth surface wear of face gear. Model change analysis step was added to remove the load deformation of tooth surface contained in the wear calculation results, while the definitions of material properties, element properties, reference points,

boundary conditions and loads of two wheels remain unchanged. Figure 2 shows the finite element mesh wear model of tooth surface drive of face gear pair.

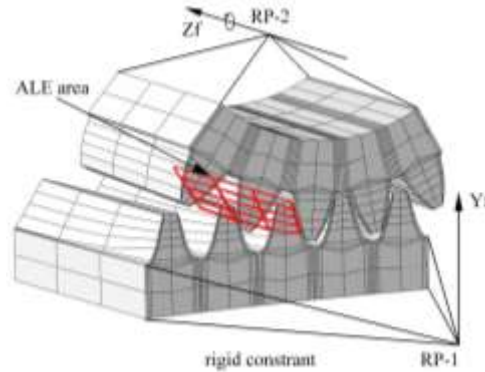


Figure 2. Finite element mesh wear model of face gear pair (unrefined mesh)

The post-processing program was written by using python language embedded in ABAQUS, and the results of tooth surface load, tooth root bending stress, tooth surface contact stress and angular displacement of pinion were obtained.

2.5 Wear simulation process

In this paper, we assumed that pinion surface hardness is large enough, so the wear of pinion was not considered. The face gear experienced 12 mesh cycles, and the wear at the sixth contact point of the face gear tooth surface reached $5 \mu\text{m}$ in each mesh cycle. So as to improve the accuracy of bearing contact problem solving, we updated face gear tooth surface when the wear calculation of each mesh circle was completed.

The nodes coordinate matrix of the observed tooth surface of face gear was obtained from the position vector of the worn tooth surface. According to the position relationship between the observed tooth surface and the other four tooth surfaces, the nodes coordinate matrix of all tooth surfaces of face gear was obtained. We wrote the worn node coordinate matrix information into txt file to update the finite element model, and the load-bearing contact problem of worn face gear pair was solved by using ABAQUS post-processing program.

In this paper, when the cumulative wear depth at the sixth contact point of face gear tooth surface reached 5, 10, 15, 20, 25, 30, 35, 40, 45, 50, 55, 60 μm , the corresponding face gear pair engagement times were 4.2×10^{10} , 9.8×10^{10} , 14.4×10^{10} , 19.4×10^{10} , 24.7×10^{10} , 30.6×10^{10} , 36.7×10^{10} , 43.2×10^{10} , 50.3×10^{10} , 57.8×10^{10} , 65.3×10^{10} and 73.9×10^{10} . The engagement times required for the maximum wear of the sixth contact point to reach $5 \mu\text{m}$ were greater than the engagement times in previous mesh circle. It was similar to the conclusion obtained by Brauer [20] in the wear analysis of cylindrical gears that the wear rate decreases slowly with the increase of engagement times.

Figure3 shows the process of wear simulation.

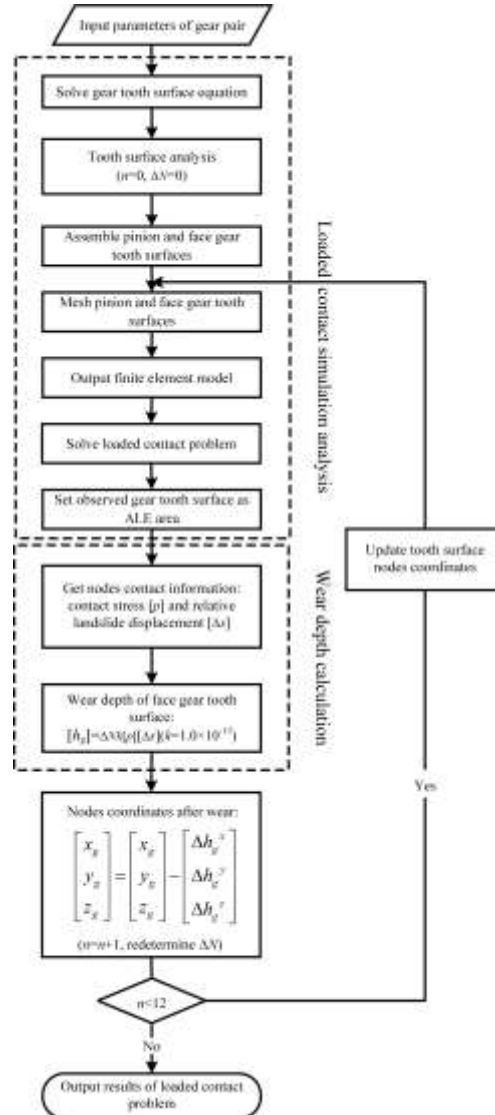


Figure3. Wear simulation process

III. Wear simulation Results

3.1 Relative sliding displacement distribution along contact path

The relative sliding displacement of each contact point was obtained by accumulating the relative sliding displacement of each incremental step output by ABAQUS UMESHMOTION subroutine. Figure4 shows the relative sliding displacement distribution of each contact point along the contact path after wear.

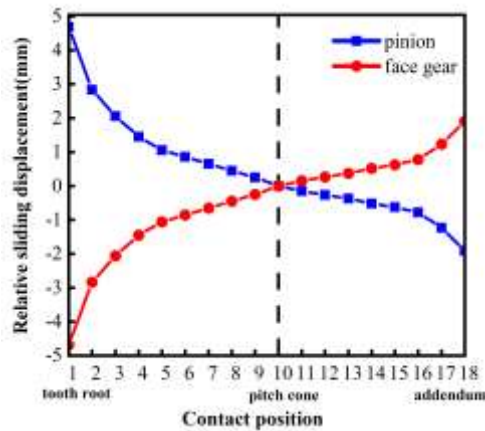


Figure4. Relative sliding displacement along the contact path

3.2 Wear distribution of face gear tooth surface

Figure5 shows the wear distribution of face gear tooth surface when the face gear pair engages 73.9×10^{10} times.

The most serious wear occurs at the tooth root, and the maximum wear depth is about $112.48 \mu\text{m}$; the maximum wear depth near the addendum is about $20.61 \mu\text{m}$; the pitch cone wear depth is almost 0. In the gear engagement process, due to the large contact stress and relative sliding displacement at the tooth root of face gear, the wear at the tooth root is the most serious. Although there is certain contact stress at the pitch cone, the wear depth is almost 0 because the relative sliding displacement is close to 0. Compared with the wear distribution of addendum, the wear distribution of tooth root is uneven. The wear law of tooth surface along the tooth width direction is approximately convex parabola, and the wear law along the tooth height direction is approximately concave parabola.

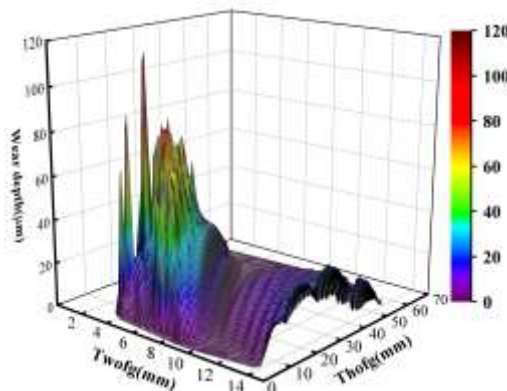


Figure5. Tooth wear distribution of surface gear

Twofg: Tooth width of face gear; Thofg: Tooth height of face gear.

3.3 Change of load-bearing contact characteristics of face gear tooth surface wear

3.3.1 load distribution coefficient among gear tooth

When the contact point is near the center of face gear pitch cone, the load distribution coefficient among teeth is the maximum. Figure6 shows the change of the maximum load distribution coefficient among teeth after wear.

When face gear pair engagement times are less than 43.2×10^{10} , that is, before the cumulative wear depth of the sixth contact point reaches $40 \mu\text{m}$, the maximum load distribution coefficient among teeth increases continuously with the increase of engagement times, indicating that the tooth surface in the pitch cone gradually bears more load. When the engagement times are greater than 43.2×10^{10} , that is, the cumulative wear depth of the sixth contact point is within the range of $40 \mu\text{m}$ to $60 \mu\text{m}$, the maximum load distribution coefficient among teeth gradually approaches the constant value with the increase of engagement times.

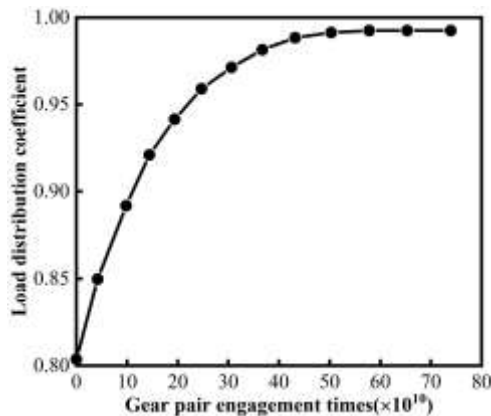


Figure6. Maximum load distribution coefficient among teeth after wear

3.3.2 gear root bending stress

When the contact point is near the center of face gear pitch cone, the tooth root bending stress of face gear and pinion is the maximum. Figure7 shows the change of maximum tooth root bending stress face gear and pinion after wear.

With the increase of gear pair engagement times, the maximum tooth root bending stress of face gear and pinion increases continuously. When the face gear pair engages 73.9×10^{10} times, the maximum tooth root bending stress of face gear is about 130.12Mpa , the maximum tooth root bending stress of pinion is about 131.59Mpa . The maximum tooth root bending stress of pinion is always greater than face gear.

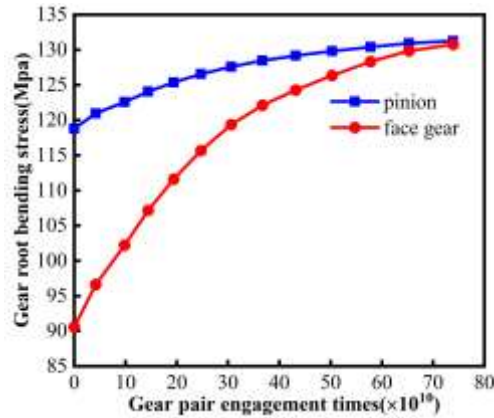


Figure7. Maximum root bending stress of face gear and pinion after wear

3.3.3 tooth surface contact stress

Figure8 shows the change of maximum contact stress at the tooth root and addendum after wear.

With the increase of gear pair engagement times, the tooth surface contact stress at addendum and tooth root decreases continuously, and the contact stress gradually approaches the constant value, indicating that appropriate tooth surface wear can improve the negative impact of excessive tooth surface contact stress caused by tooth edge contact.

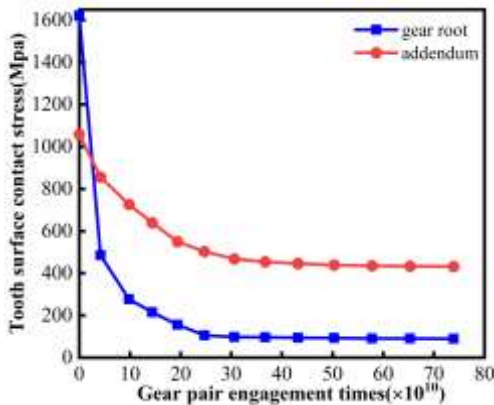


Figure8. Maximum tooth surface contact stress at the tooth root and addendum after wear

Figure9 shows the change of maximum tooth surface contact stress at the pitch cone after wear.

When face gear pair engagement times are less than 43.2×10^{10} , that is, before the cumulative wear depth of the sixth contact point reaches $40\mu\text{m}$, tooth surface contact stress at pitch cone increases continuously. When the engagement times are greater than 43.2×10^{10} , that is, the cumulative wear depth of the sixth contact point is within the range of $40\mu\text{m}$ to $60\mu\text{m}$, contact stress decreases slightly and approaches the constant value gradually with the increase of engagement times.

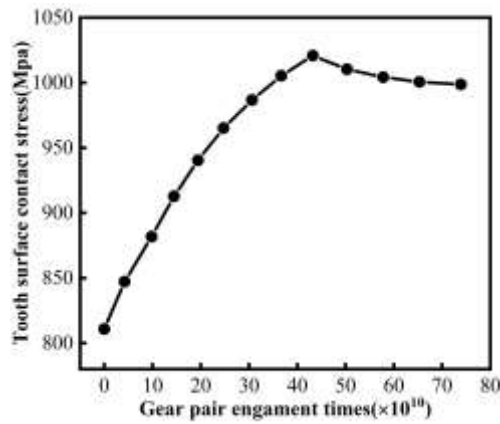


Figure9. Maximum tooth surface contact stress at the pitch cone after wear

3.3.4 loaded transmission error

Figure. 10 shows the change of the amplitude value and mean value of loaded transmission error after wear.

With the increase of face gear pair engagement times, the amplitude value and mean value of loaded transmission error increase continuously. When the face gear pair engages 73.9×10^{10} times, the amplitude value of loaded transmission error is about $4.31''$, and the mean value is about $-12.83''$.

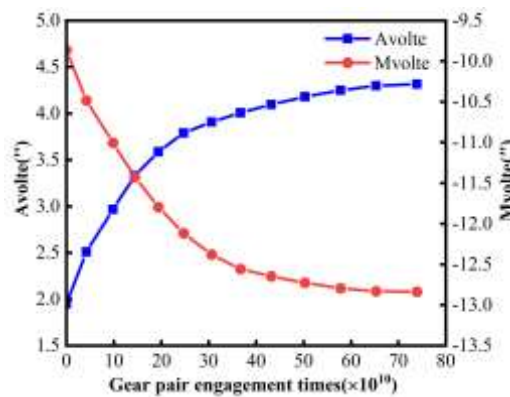


Figure10. Amplitude value and mean value of loaded transmission error

Avalte: Amplitude value of loaded transmission error; Mvalte: Mean value of loaded transmission error

IV. Conclusion

In order to study the wear mechanism of face gear tooth surface, based on tooth contact analysis (TCA) numerical

method and Archard wear theory, the UMESHMOTION subroutine in ABAQUS was developed, combining with ALE adaptive mesh technology, the finite element mesh wear model of face gear pair was established. The tooth surface wear distribution of face gear was calculated, and the load-bearing contact

problem of worn face gear pair was solved. The conclusions are as follows:

The most serious wear occurs at the tooth root and the pitch cone wear depth is almost 0. The wear law of tooth surface along the tooth width direction is approximately convex parabola, and the wear law along the tooth height direction is approximately concave parabola. In order to decrease wear at tooth root, the stub gear tooth can be selected.

With the increase of gear pair engagement times, the pitch cone tooth surface bear more loads. In order to avoid gear tooth failure, it can be considered to increase the surface hardness of pitch cone. With the increase of gear pair engagement times, tooth root bending stress of face gear and pinion increases continuously. In order to avoid the local deformation of gear tooth caused by the increase of bending stress, it can be considered to increase the gear tooth thickness. With the increase of gear pair engagement times, the tooth surface contact stress at addendum and tooth root decreases continuously, and the contact stress gradually approaches the constant value. Moderate tooth surface wear improves the bearing contact performance of face gear.

With the increase of gear pair engagement times, the amplitude value and mean value of loaded transmission error increase continuously, indicating that the bearing stiffness of gear tooth decreases continuously, the impact vibration and bearing deformation of gear tooth increase continuously.

ACKNOWLEDGE

Natural Science basic Research Project of China Shaanxi Province(2020JM-521)

REFERENCES

- [1] ASSAG. Cylkro face gears dutch design and swiss ingenuity cause transmission breakthrough [Z]. Dudingen Switzerland: Gear Technology, 2010.
- [2] FLODIN A, ANDERSSON S. Wear simulation of spur gears[J]. Tribotest, 1999, 5(3): 225-249.
- [3] FLODIN A, ANDERSSON S. Simulation of mild wear in helical gears[J]. Wear, 2000, 241(2) : 123-128.
- [4] FLODIN A, ANDERSSON S. A simplified model for wear prediction in helical gears[J]. Wear, 2001, 249(3) : 285-292.
- [5] ZHU Lisha, XIANG Lei, ZOU Changqing. Wear analysis of gears under dynamic load distribution between gear teeth[J]. Journal of Xi'an Jiao Tong University, 2018, 52(5): 80-85.
- [6] ZHANG Jiange, LIU Shaojun, FANG Te. Prediction of gear wear rate in mixed lubrication and experimental verification[J]. Journal of South China University of Technology (Natural Science Edition), 2018, 46(2): 22-30.
- [7] ZHOU Changjiang, WANG Hongbing, LEI Yuying, et al. Calculating and measuring methods for gear wear and its suppression techniques[J]. Journal of Beijing University of Technology, 2018, 44(7): 987-1000.
- [8] PAN Dong, ZHAO Yang, LI Na, et al. The wear life prediction method of gear system[J]. Journal of Harbin Institute of Technology, 2012, 44(9): 29-33, 39.
- [9] S. Khalilpourazary & S. S. Meshkat (2014) Investigation of the effects of alumina nanoparticles on spur gear surface roughness and hob tool wear in hobbing process. International Journal of Advanced Manufacture Technology 71: 1599-1610. doi:10.1007/s00170-013-5591-8
- [10] JANAKIRAMAN V, LI S, KAHRAMAN A. An investigation of the impacts of contact parameters on wear

coefficient[J]. *Journal of Tribology*,2014,136(3):031602.

- [11] Zhe Yuan , Yuhou Wu, Ke Zhang,et al. Wear reliability of spur gear based on the cross[J].*Advances in Mechanical Engineering*,2018,Vol.10(12).
- [12] Park D, Kahraman A. A surface wear model for hypoid gear pairs. *Wear*, 2009, 267(9):1595-1604.
- [13] Park D,Kolivand M, Kahraman A. A prediction of surface wear of hypoid gears using a semi-analytical contact model. *Mechanism and Machine Theory*, 2012, 52:180-194.
- [14] Park D, Kolivand M, Kahraman A. An approximate method to predict surface wear of hypoid gears using surface interpolation. *Mechanism and Machine Theory*, 2014, 71:64-78.
- [15] HOU Xiangying, FANG Zongde, DENG Xiaozhong, et al. Contact analysis of spiral bevel gears based on finite element mode[J]. *Journal of Harbin Engineering University*,2015,36(6):826—830.
- [16] PENG Xianlong, XU Qichao, HOU Xiangying, KOU Farong. Finite element analysis of gear bearing transmission performance influenced by misalignment[J]. *Journal of Harbin Engineering University*,2020,41(12):1861-1867.
- [17] LITVIN F L.Gear geometry and applied theory[M]Cambridge: Cambridge University Press,1994: 490-523.
- [18] ARCHARD J F. Contact and rubbing of flat surfaces[J]. *Journal of Applied Physics*,1953,24(8):981-988.
- [19] Bose K K, Penchaliah R. 3-D FEM wear prediction of brass sliding against bearing steel using constant contact pressure approximation technique[J]. *Tribology*, 2019, 14(4): 194-207.
- [20] Brauer J, Andersson S. Simulation of wear in gears with flank interference: a mixed FE and analytical approach[J].*Wear*, 2003, 254(11): 1216-1232.